

Vacancy-tuned paramagnetic/ferromagnetic martensitic transformation in Mn-poor $\text{Mn}_{1-x}\text{CoGe}$ alloys

E. K. Liu, W. Zhu, L. Feng, J. L. Chen, W. H. Wang, and G. H. Wu^{*}

Beijing National Laboratory for Condensed Matter Physics, Institute of Physics, Chinese Academy of Sciences, Beijing 100190, China

H. Y. Liu, F. B. Meng, H. Z. Luo, and Y. X. Li

School of Material Science and Engineering, Hebei University of Technology, Tianjin 300130, China

A temperature window between the Curie temperatures of martensite and austenite phases around the room temperature is obtained by our vacancy-tuning strategy in Mn-poor $\text{Mn}_{1-x}\text{CoGe}$ alloys ($0 \leq x \leq 0.050$). Based on this, a martensitic transformation from paramagnetic austenite to ferromagnetic martensite is realized in this window with a large magnetization difference of about 70 emu/g. This subsequently confers the magnetic-field-induced martensitic transformation and large magnetocaloric effect on $\text{Mn}_{1-x}\text{CoGe}$ system. With regard to the decreases of transformation temperature and thermal hysteresis of martensitic transformation, the corresponding thermodynamic nature is discussed on the basis of the Mn-poor Co-vacancy structure.

Keywords: martensitic transformation; magnetic transition; ferromagnetic shape memory alloy; magnetocaloric effect; MnCoGe

^{*} Author to whom correspondence should be addressed; electronic mail: ghwu@aphy.iphy.ac.cn

Stoichiometric MnCoGe crystallizes in the hexagonal Ni₂In-type structure (austenite, *A*) and undergoes a martensitic transformation (MT) to the orthorhombic TiNiSi-type structure (martensite, *M*) at 420 K.¹⁻³ The two phases are collinear ferromagnets⁴⁻⁵ with the Curie temperatures (T_C^A and T_C^M) of 273 and 355 K,²⁻³ respectively. The magnetic moment of *M* phase is larger than that of *A* one.^{2,6} Recently, it has been found that the vacancies of transition metal Co can decrease the martensitic transformation starting temperature (T_m) and T_C of MnCoGe system.⁷⁻¹⁰ If the T_m could be decreased while the T_C^A and T_C^M could be kept steady, a special MT from the paramagnetic (PM) *A* to ferromagnetic (FM) *M*, similar to that in MnCoGe_{1-x}Sn_x¹¹ and Fe₂MnGa¹²⁻¹³ systems, can be obtained inside the temperature window constructed by the T_C^A and T_C^M . This may afterwards cause a large difference of magnetization (ΔM) between the two phases and a consistence in exothermic/endothermic behaviors of the magnetic and structural transitions, which is of foremost importance for some functional applications such as magnetic-field-induced sensors and magnetocaloric materials.

In MnCoGe system, however, only the FM/FM-type MT with relatively small ΔM in Co-poor alloy has been reported⁷ and, the temperature window as well as resultant PM/FM-type MT tuned by transition metal vacancies is still unexposed. Very recently, we utilize the vacancy-tuning strategy via Mn-poor Co-vacancy method and obtain this temperature window at room-temperature region; meanwhile, the T_m is tailored into this window. In this letter, the desired PM/FM-type martensitic transformation with a quite large ΔM in Mn-poor Mn_{1-x}CoGe alloys is realized.

From a high-temperature XRD study¹⁴ on $\text{Mn}_{0.98}\text{CoGe}$ compound, it can be known that partial Co atoms occupy the Mn-deficient sublattices and vacancies at Co sublattices form instead. In this study, for $\text{Mn}_{1-x}\text{CoGe}$ system, we consider the Mn-vacancy and Co-vacancy structures and calculate their total energies using *ab initio* method. The results confirm the Co-vacancy structure, $(\text{Mn}_{1-x}\text{Co}_x)(\text{Co}_{1-x}\square_x)\text{Ge}$, is energetically favored. We thus attempt to take advantage of this Co-vacancy structure by properly reducing Mn content to tune the phase transition behaviors of present $\text{Mn}_{1-x}\text{CoGe}$ alloys. One can see that the Co vacancy content equals to the deficient level (x) of Mn in the $\text{Mn}_{1-x}\text{CoGe}$ alloys.

Polycrystalline ingots of $\text{Mn}_{1-x}\text{CoGe}$ ($x=0, 0.010, 0.020, 0.030, 0.035, 0.045$ and 0.050) are prepared by arc-melting raw metals in high-purity argon atmosphere. The ingots are annealed at 1123 K for 5 days and quenched in cool water. The crystal structures of specimens are identified by powder x-ray diffraction (XRD) analysis with Cu $K\alpha$ radiation. Magnetization measurements are carried out on a superconducting quantum interference device (SQUID). The differential thermal analysis (DTA) method with heating and cooling rates of 2.5 K/min is also used to measure the martensitic transformation data.

Fig. 1 shows the XRD patterns obtained at the different temperatures for the alloy with $x=0.035$. At 320 K, the Ni_2In -type structure is detected with the lattice parameters of $a=4.0846$ and $c=5.3093$ Å. At 220 K, the Bragg peaks of TiNiSi -type structure are well indexed with the lattice parameters of $a=5.9638$, $b=3.8294$ and $c=7.0626$ Å. The unit cell volume increases by 5.6%, which means a tremendous

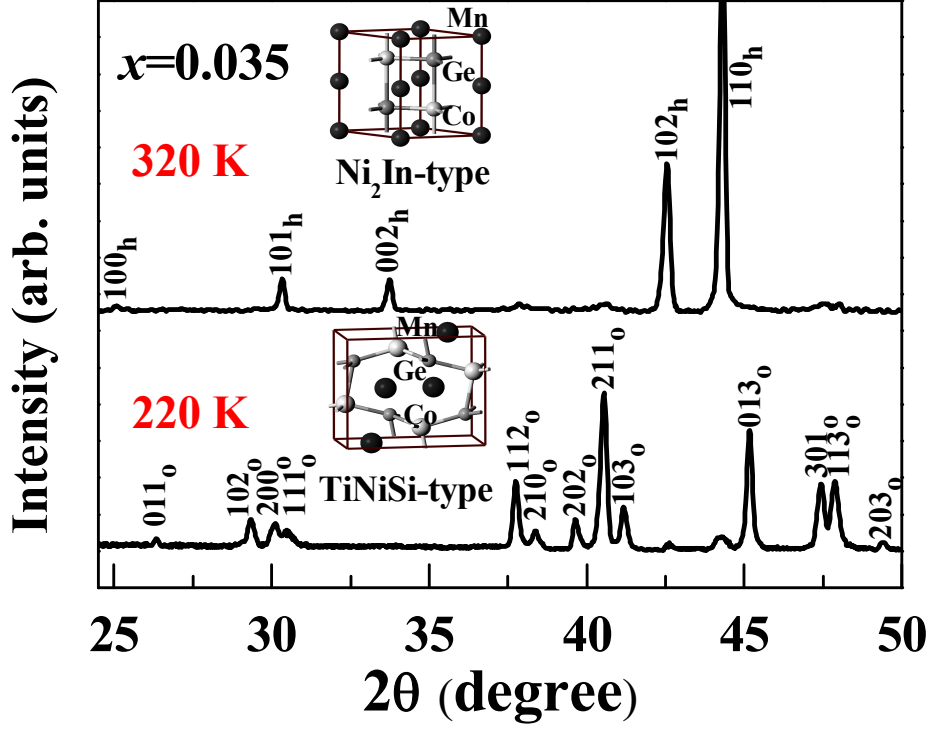


Fig. 1. (Color online) Power XRD patterns of the alloy with $x=0.035$ at 320 and 220 K on cooling. The Miller indices of hkl_h and hkl_o denote the hexagonal and orthorhombic structures, respectively. The unit cells of both structures are also shown.

lattice distortion during the transformation. The crystal structures of both phases are also shown in Fig. 1. Our XRD examinations at room temperature (not shown) confirm that the alloys with the compositions of $x=0 \sim 0.045$ share the MT behavior and their T_m regularly decreases through the room-temperature region. This indicates that the T_m in $Mn_{1-x}CoGe$ is sensitive to the Mn deficient-level (x) and it could be tailored to a desired temperature by our vacancy-tuning strategy.

Fig. 2(a) shows the $M(T)$ curves of $Mn_{1-x}CoGe$ ($x = 0.010, 0.030, 0.035$ and 0.045) alloys in a low magnetic field of 0.01 T and the characteristic parameters of T_m , T_C and thermal hysteresis (ΔT) are listed in Table I. In Fig. 2(a), the T_C^M (353 K) shown on right-hand side corresponds to the Curie temperature of M phase for the alloy with vacancy content $x = 0.010$, while the T_C^A (261 K) on left-hand side corresponds to

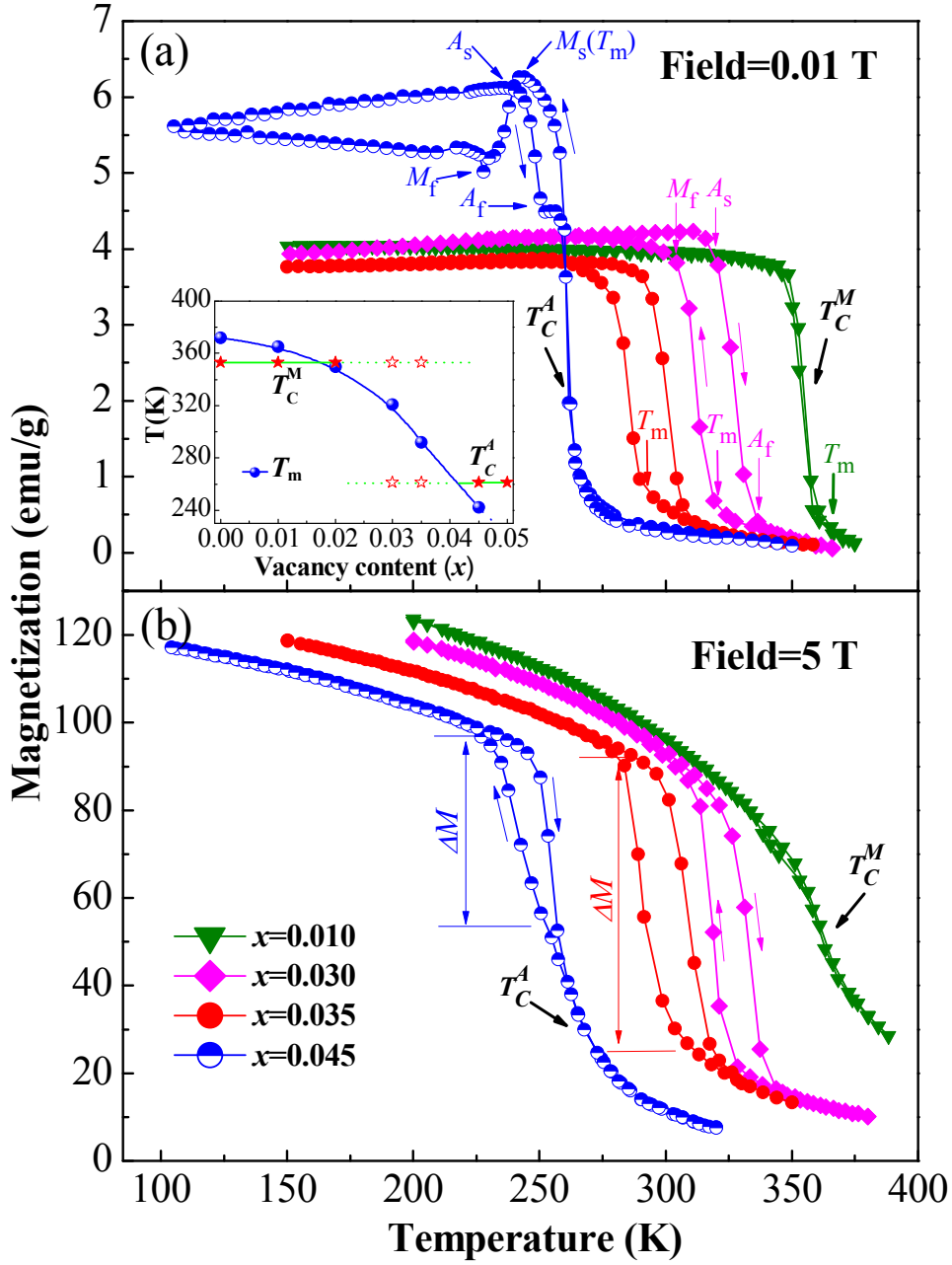


Fig. 2. (Color online) Temperature dependence of the magnetization of $\text{Mn}_{1-x}\text{CoGe}$ ($x=0.010$, 0.030 , 0.035 and 0.045) alloys in the fields of 10 mT (a) and 5 T (b), respectively. The $M_s(T_m)$, M_f , A_s and A_f denote the martensitic transformation starting, finishing, reverse transformation starting and finishing temperatures, while the T_C^A and T_C^M denote Curie temperatures of A and M , respectively. Inset is the phase diagram for these four compositions. The solid pentacles denote the measured T_C and open pentacles the deduced T_C for clarity.

that of A phase for the alloy with vacancy content $x = 0.045$. As the left and right borders respectively, the T_C^M and T_C^A thus together construct a temperature interval.

It can be seen that the martensitic transformations of these two alloys, occurring at 365 K and 242 K (see Table I) respectively, are both outside the interval. The further measurements of the alloys with $x=0$ and 0.020 show that their T_C^M are both situated at the right border temperature. Similarly, the T_C^A of alloy with $x = 0.050$ coheres with the left border temperature. This reveals an instinct character that both T_C of martensite and austenite are insensitive to Mn deficient-level (x) of $\text{Mn}_{1-x}\text{CoGe}$ system in range of $x = 0 \sim 0.050$. Thus, there is a stable temperature window with a width of about 100 K between the T_C^M and T_C^A in Mn-poor $\text{Mn}_{1-x}\text{CoGe}$ system. Collecting these results, a phase diagram for $\text{Mn}_{1-x}\text{CoGe}$ system ($0 \leq x \leq 0.050$) is further proposed in the inset to Fig. 2(a). With the vacancy content further optimized into the range of $0.010 < x < 0.045$, the alloys display first-order martensitic transformation behaviors from PM A phases to FM M phases. Two alloys with vacancy content $x = 0.030$ and 0.035 are shown in the Fig. 2(a). During cooling, the A phase of each alloy transforms to M phase above the T_C^A and the T_C^A thus becomes

TABLE I. Composition dependence of T_m , T_C , ΔM and ΔT for $\text{Mn}_{1-x}\text{CoGe}$ alloys.

| x | $T_m(\text{K})$ | $T_C(\text{K})$ | $\Delta M(\text{emu/g})$ | $\Delta T(\text{K})$ |
|------------------|-----------------|-----------------|--------------------------|----------------------|
| 0.000* | 372 | 353 | - | 29 |
| 0.010* | 365 | 353 | - | 22 |
| 0.020** | 350 | 353 | 73 | 19 |
| 0.030*** | 321 | - | 70 | 16 |
| 0.035*** | 292 | - | 71 | 15 |
| 0.045 | 242 | 261 | 41 | 12 |
| 0.050**** | - | 261 | - | - |

* The T_m and ΔT are determined using DTA as the transformation occurs at the temperature range where the system is in the paramagnetic state. The ΔM are absent due to the same reason.

** The data of this alloy are determined using DTA and magnetic measurements as its transformation is situated at the T_C of martensite.

*** The T_C are immeasurable due to the PM/FM-type MT behaviors of these two alloys.

****The T_m , ΔM and ΔT are absent as the MT behavior of this alloy disappears.

nonexistent. During heating, likewise, the M phase inversely transforms to A phase below the T_C^M and the T_C^M is also nonexistent. For clarity, we validly mark their T_C^A and T_C^M on the window borders by open pentacles (☆), though they are immeasurable.

The thermomagnetization of samples in high field of 5 T is shown in Fig. 2(b). The corresponding ΔM across the MT are listed in Table I. In contrast to the other alloys, the alloys in the window exhibit abrupt increments of magnetization due to the transformation from PM A to FM M and their ΔM s reach up to about 70 emu/g. This value is much larger than that (about 31.7 emu/g) of Co-poor MnCoGe alloy across an FM/FM-type MT.⁷ For the left-border alloy, as the transformation decreases out of the window, the ΔM immediately reduces to only about 41 emu/g after the spontaneous magnetization of its A phase. It can be seen that the T_m shifts toward to the high-temperature region due to the high magnetism of FM M phase relative to the PM A one.

According to the results above, it is clearly observed that the phase transition behaviors in the materials strongly correlate with the Co vacancy contents. In MnCoGe system, the Co and Ge atoms structure three-dimensional chain networks via covalent bonds owing to the sp and sd orbital hybridizations.^{3, 15-16} These chemical bonds significantly contribute to the binding energy of M phase.¹⁷ The existence of Co vacancies in Co-Ge-Co chains destroys the consecutive distribution of chemical bonds¹⁸ and might cause a consequent decrease in binding energy of M phase, which results in the lattice destabilization and its transformation at lower temperature into

the high-temperature energy-stabilized hexagonal A phase. Also, this vacancy defect in $\text{Mn}_{1-x}\text{CoGe}$ alloys will weaken the elastic modulus of A phase¹⁹ and, accordingly, the system possesses a decreased shearing strain energy.²⁰ The phase transformation thus needs a decreased thermodynamic driving force for overcoming the energy barrier of its M nucleation.²¹⁻²³ As shown in Table I, the ΔT of MT in troth exhibits a decreasing trend, from 22 to 12 K, as a function of increasing vacancy content. In consequence, the Co vacancies induce regular decreases of both T_m and ΔT of transformation in $\text{Mn}_{1-x}\text{CoGe}$ alloys, accompanying a series of abundant magnetic behaviors.

Considering the large ΔM across the transformation of the alloys in the window, we give the isothermal $M(H)$ curves of alloy with $x=0.035$ in the field up to 13 T on cooling, as depicted in Fig. 3. From 300 down to 285 K, the metamagnetic phase

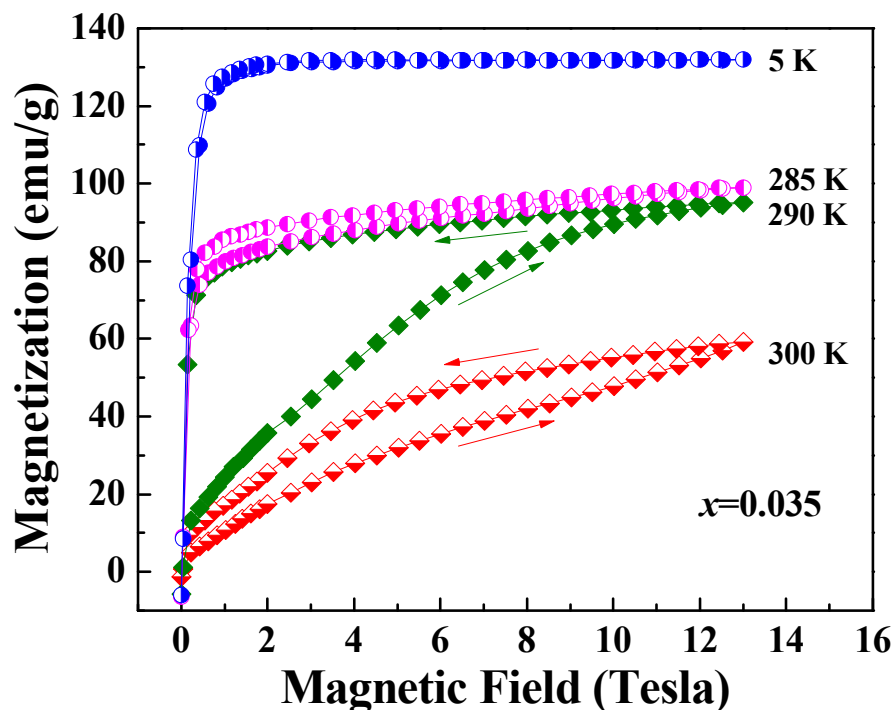


Fig. 3. (Color online) Isothermal magnetization curves of the alloy with $x=0.035$ at various given temperatures across the MT.

transition with hysteresis indicates the magnetic-field-induced MT happens in this temperature region with the contribution of Zeeman energy between PM A and FM M phases due to the distinct ΔM . At 5 K, the curve shows a typical ferromagnetic magnetization behavior of M , exhibiting a high saturation magnetization of 131.9 emu/g.

As shown in Fig. 4, the magnetocaloric effect is measured using the magnetizing curves over a field span of 5 T for the alloy with $x=0.035$. Around the T_m , the large and negative ΔS_m values (-10 J/kg·K at 2 T and -26 J/kg·K at 5 T) are observed. These values are to some extent comparable with those of some other materials in similar temperature range, such as $\text{Gd}_5(\text{Si}_2\text{Ge}_2)$ (-14 J/kg·K at 2 T)²⁴ and $\text{Ni}_{50}\text{Mn}_{33.13}\text{In}_{13.90}$ (-28.6 J/kg·K at 5 T).²⁵ It can be seen that the $\text{Mn}_{1-x}\text{CoGe}$ alloys in the range of 0.010

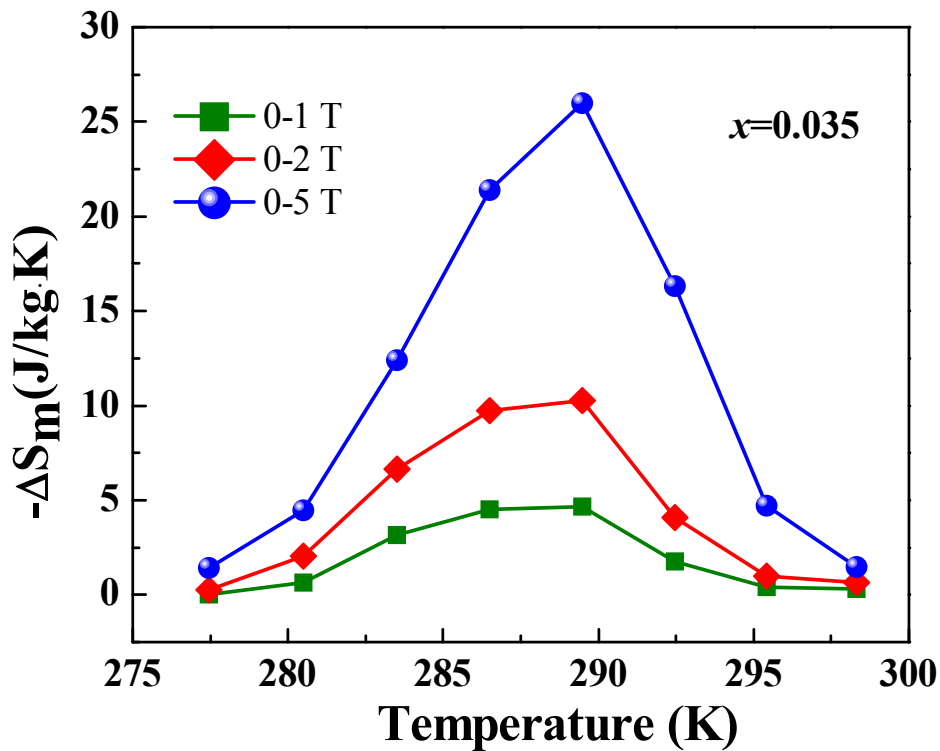


Fig. 4. (Color online) Isothermal magnetic entropy changes calculated using the magnetizing curves of the alloy with $x=0.035$ in different applied fields.

$x < 0.045$ show a considerable magnetocaloric effect at room temperature, though the corresponding properties can be further improved. It should be emphasized that, for the alloys in the window, the exothermic/endothermic effect of the magnetic entropy change is consistent with that of the martensitic structural transformation, which can be regarded as an enhanced thermal effect.

In summary, a stable temperature window between T_C^A and T_C^M is reported in Mn-poor $\text{Mn}_{1-x}\text{CoGe}$ alloys with Co vacancy content in range of $0.010 < x < 0.045$ and the vacancy-tuned PM/FM-type martensitic transformation with large ΔM is resultantly realized. This confers new physical characters and promising functions on MnCoGe system. In this study, the field-induced martensitic transformation and large magnetocaloric effect in these Mn-poor $\text{Mn}_{1-x}\text{CoGe}$ alloys are observed.

This work is supported by National Natural Science Foundation of China in Grant No. 50531010 and 50771103.

References

- ¹L. Castelliz, *Mon. Chem.* **84**, 765 (1953).
- ²V. Johnson, *Inorg. Chem.* **14**, 1117 (1975).
- ³S. Niziol, A. Weselucha, W. Bazela, and A. Szytula, *Solid State Commun.* **39**, 1081 (1981).
- ⁴A. Szytula, A. T. Pedziwiatr, Z. Tomkowicz, and W. Bazela, *J. Magn. Magn. Mater.* **25**, 176 (1981).
- ⁵S. Niziol, A. Bombik, W. Bazela, A. Szytula, and D. Fruchart, *J. Magn. Magn. Mater.* **27**, 281 (1982).
- ⁶S. Kaprzyk, and S. Niziol, *J. Magn. Magn. Mater.* **87**, 267 (1990).
- ⁷K. Koyama, M. Sakai, T. Kanomata, and K. Watanabe, *Jpn. J. Appl. Phys. Part 1* **43**, 8036 (2004).
- ⁸J. T. Wang, D. S. Wang, C. F. Chen, O. Nashima, T. Kanomata, H. Mizuseki, and Y. Kawazoe, *Appl. Phys. Lett.* **89**, 262504 (2006).
- ⁹P. E. Markin, N. V. Mushnikov, V. I. Khrabrov, and M. A. Korotin, *Phys. Metals Metallogr.* **106**, 481 (2008).
- ¹⁰Y. K. Fang, J. C. Yeh, W. C. Chang, X. M. Li, and W. Li, *J. Magn. Magn. Mater.* **321**, 3053 (2009).
- ¹¹J. B. A. Hamer, R. Daou, S. Özcan, N. D. Mathur, D. J. Fray, and K. G. Sandeman, *J. Magn. Magn. Mater.* **321**, 3535 (2009).
- ¹²T. Omori, K. Watanabe, R. Y. Umetsu, R. Kainuma, and K. Ishida, *Appl. Phys. Lett.* **95**, 082508 (2009).
- ¹³W. Zhu, E. K. Liu, L. Feng, X. D. Tang, J. L. Chen, G. H. Wu, H. Y. Liu, F. B. Meng, and H. Z. Luo, *Appl. Phys. Lett.* **95**, 222512 (2009).
- ¹⁴W. Jeitschko, *Acta Crystallogr. B, Struct. Crystallogr. Cryst. Chem.* **B31**, 1187 (1975).
- ¹⁵Shoemaker.Cb, and Shoemaker.Dp, *Acta Crystallogr* **18**, 900 (1965).
- ¹⁶G. A. Landrum, R. Hoffmann, J. Evers, and H. Boysen, *Inorg. Chem.* **37**, 5754 (1998).
- ¹⁷V. Johnson, and W. Jeitschk, *J. Solid State Chem.* **4**, 123 (1972).
- ¹⁸A. H. Cottrell, *Intermetallics* **3**, 341 (1995).
- ¹⁹A. Cano, and A. P. Levanyuk, *Phys. Rev. B* **62**, 12014 (2000).
- ²⁰X. Wang, and J. Zhang, *Acta Mater.* **55**, 5169 (2007).
- ²¹S. Kartha, J. A. Krumhansl, J. P. Sethna, and L. K. Wickham, *Phys. Rev. B* **52**, 803 (1995).
- ²²B. Li, X. M. Zhang, P. C. Clapp, and J. A. Rifkin, *J. Appl. Phys.* **95**, 1698 (2004).
- ²³Z. Zhang, R. D. James, and S. Müller, *Acta Mater.* **57**, 4332 (2009).
- ²⁴V. K. Pecharsky, and J. K. A. Gschneidner, *Phys. Rev. Lett.* **78**, 4494 (1997).
- ²⁵X. X. Zhang, B. Zhang, S. Y. Yu, Z. H. Liu, W. J. Xu, G. D. Liu, J. L. Chen, Z. X. Cao, and G. H. Wu, *Phys. Rev. B* **76**, 132403 (2007).